18TH WORLD CONFERENCE ON EARTHQUAKE ENGINEERING
WCEE2024
MILAN

MILAN, ITALY
30TH JUNE - 5TH JULY 2024
www.wcee2024.it

STUDY OF VALLEY EFFECTS IN GÖKSUN DISTRICT (TÜRKIYE) DURING THE 6TH FEBRUARY EARTHQUAKES

T. Oktay Gul[1], E. Karakan[2], A. Sezer[3], A. Chiaradonna[4], C. Kincal[5], M. Karray[6], G. Lanzo[7] & P. Monaco[8]

[1,6] Université de Sherbrooke, Québec, Canada, gul.tolga.oktay@usherbrooke.ca

[2] Kilis 7 Aralik University, Kilis, Türkiye

[3] Ege University, Izmir, Türkiye

[4,8] University of L'Aquila, L'Aquila, Italy

[5] Dokuz Eylul University, Izmir, Türkiye

[7]Sapienza University of Rome, Rome, Italy

Abstract: *Two successive devastating earthquakes occurred in Eastern Türkiye on the 6th of February 2023. The epicenter of the Pazarcik earthquake was 45 km west of the city of Gaziantep, with a depth and moment magnitude of the event are 8.6 km and 7.7, respectively. A second event (Elbistan) occurred 66 km northeast of Kahramanmaras just nine hours after the first. The second event's depth was 7 km, and its moment magnitude was 7.6.*

The characteristics of ground motion distribution during these events were unusual. The epicenter of the first event triggered the Eastern Anatolian fault system, producing surface shear ruptures surpassing 300 km. On the other hand, the Elbistan earthquake showed a more expected behavior, with seismic movements presenting an attenuating behavior. Göksun city and the periphery were an exception here, while the city is embedded in a valley, and the distance between the city and the epicenters of the first and second events were 68.66 km and 95.6 km, respectively. The maximum acceleration recorded at the 4612 station was about 0.815 g and 0.144 g for the Elbistan and Pazarcik earthquakes, respectively.

In this paper, in-depth analyses were carried out to study the valley effects produced during the 6th of February earthquakes in Göksun. The results of analyses clearly prove the role of the site effects during these events. These site effects, accompanied with the very low quality of the building stock, were the reasons for widespread destruction and damage.

1. Introduction

On February 6th, 2023, the southeastern region of Türkiye, including the city of Göksun was shaken by two consecutive catastrophic earthquakes with moment magnitudes (M_w) of 7.7 and 7.6, as reported by the Disaster and Emergency Management Presidency - AFAD (AFAD, 2023a). The magnitudes of the two events declared by the United States Geological Survey – USGS were M_w=7.8 and 7.5, respectively.

The region where the events of February 6th, 2023 took place is the connection of two major active strike-slip fault systems in the Middle East. Most of the influenced settlement areas and the environment are formed of mountains, valleys and sedimentary basins. It is evident that local soil conditions and, to a certain extent, irregularities in surface and subsurface geology can significantly influence the extent of building damage as well as spatial distribution during ground shaking. Basin and valley effects play a remarkable role in the amplification of seismic ground motions since two-dimensional (2D) and three-dimensional (3D) effects

become more pronounced by topography effects and resilient materials confining valleys. Bard and Bouchon (1980a,b; 1985), the pioneers in pronouncing the effects of 2D sedimentary valleys, revealed that the finite lateral extent of the surface layers causes amplifying or deamplifying effects with reference to the one-dimensional (1D) theory, including the formation of surface waves at the limits of the valleys and the interaction among surface waves and incident body waves. Defined as basin effects, the interaction of seismic waves generally changes the amplitude, frequency, and duration of earthquake motion, which unfortunately affects the built environment.

An example of basin effects was shown by Seed et al. (1972) to analyze the distribution of damage in the built environment in the Caracas Valley during the 1967 earthquake, yet the magnitude was 6.4 and the epicenter was 60 km away from Caracas. Taking 1D results as a reference, a numerical study by Papageorgiou and Kim (1991) in the Caracas Valley revealed that the predicted 2D amplifications were in better agreement with the damage distribution during the 1967 earthquake. Mexico City was shaken by the Michoacan earthquake (M_w = 8.0) in 1985, which provided important information about basin effects (Garini, 2020). It should be noted that basin-edge effects, reverberation, and the amplification of seismic waves within sedimentary and highly plastic clay deposits cause these phenomena (Seed et al., 1988). Other examples including effect of the 1974 Peru earthquake (M_w=8.1) on Lima, 1988 Armenian earthquake (M = 6.8) on Kirovakan and Leninakan, 1989 Loma Prieta (M = 7.1) on Marina District, 2015 Gorkha earthquake on Kathmandu Valley (M = 7.8), and Kaikōura (M = 7.8) on Wellington (Zahradink and From, 1987; Graves et al., 1993; Yegian et al, 1994; Zhang and Papageorgiou, 1996; Bielak et al., 1999; Stephenson et al., 2009; Asimaki et al., 2017; Pagliaroli et al, 2018). A recent incidence of effects of the Samos earthquake on Bornova Basin in Izmir (Türkiye) province, which is 70 km from the epicenter, as reported by the authors, considering evidence of basin effects by analyzing ground motion characteristics and the high distribution of damage incurred. Increased amplifications in surface and prolonged ground shaking in the sedimentary Bornova basin, were associated with life and property losses in earthquake (Makra et al., 2021; Çetin et al., 2022a, 2022b; Chiaradonna et al., 2023).

Valley effects play a significant role in amplifying seismic ground motions in Göksun and its vicinity, characterized by mountainous terrain, valleys and sedimentary basins. Local soil conditions and changes in surface and subsurface geology greatly influence the extent of building damage and the spatial distribution of ground shaking in this region. The interaction between topography and resilient materials within valleys emphasizes two-dimensional (2D) and three-dimensional (3D) effects, further aggravating the impact of seismic activities on the built environment.

In this study, we focus on Göksun city and its related seismological and geological settings in the conclusion of the February 6th, 2023 earthquakes. We aim to analyze the distribution of ground motion characteristics for the two consecutive events in Göksun city and its surroundings, with a particular emphasis on assessing the observed damage and understanding the implications of basin effects in this specific geographic context.

2. The Göksun district

Göksun is a district situated in the Kahramanmaras province, within the Mediterranean region of Türkiye. The district's central area, positioned to the west of the tectonically regulated Göksun-Afsin-Elbistan basin, is located on the Göksun plain, which is encompassed by mountain ranges extending from the southern, northern, eastern, and western directions. These mountain ranges are considered as extensions of the Taurus Mountains. The Göksun Plain stretches in a northeast-southwest direction, with a length of 30 kilometers and a north-south width of 20 kilometers (Ilbank, 2010).

Göksun and its vicinity represent a region characterized by the convergence of diverse tectonic structures and significant tectonic activity. This area falls under the influence of the northern branch of the East Anatolian Fault, situated west of Celikhan, while simultaneously lying within the reach of the southern branch of the fault. The Göksun Plain, characterized by plateaus situated at an elevation of 1340 meters, has been gradually filled with alluvial deposits. These areas containing alluvial sediments extend extensively alongside riverbeds as one progresses toward the north and northeast (Figure 1).

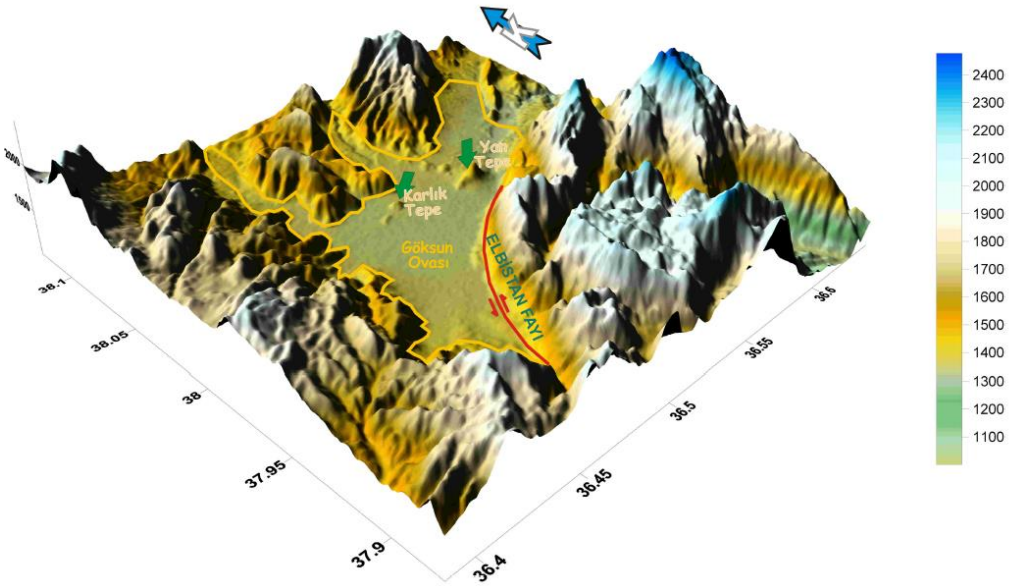

Figure 1. Three-dimensional color surface view of Göksun district (Ilbank, 2010)

2.1. Geological settings

The district of Göksun is located to the west of the tectonically controlled Göksun-Afsin-Elbistan basin. The Göksun plain, where the district center is situated, is surrounded by mountains such as Dibek, Binboga, Berit, and Armutyucesi, which are extensions of the Taurus Mountains, from the south, north, east, and west. The Göksun plain, extending in a northeast-southwest direction, covers an area of approximately 600 square kilometers.

The mountainous regions, predominantly composed of limestone, crystalline limestone, and schists, have acquired a plateau-like character through various erosion processes. The durability of these rock types, combined with steep slopes, deep incised river valleys, ridges, and peaks, has contributed to the development of a rugged and challenging topography Göksun Plain consists of flatlands with a slight southward slope (0-3°), filled with alluvial sediments of gravel, sand, silt, and clay sizes. These sediments, deposited by rivers, are unconsolidated and exhibit lateral and vertical transitions. Flood sediments from rivers are common on the plain's surface, swamp sediments have also been observed in some areas. The static water level was measured to vary between 0.1 to 4.5 meters in different boreholes throughout the Göksun plain. Particularly in the fill areas where Göksun city center is situated, the groundwater level varies between 1 to 2 meters. (Ilbank, 2010).

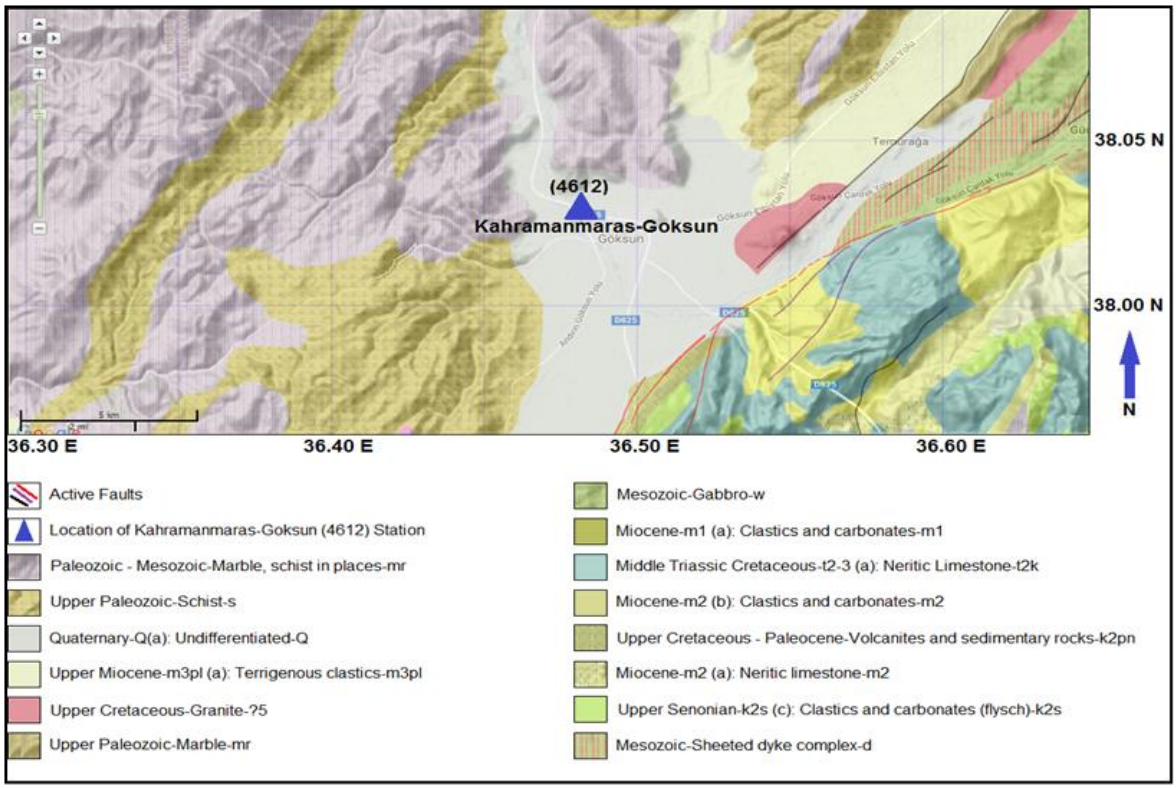

Figure 2. Station 4612 location and geological context (Emre et al., 2013)

Metamorphic rocks form the basement rocks in Göksun which include gneisses, schists, and granitic intrusions. The region also is covered by sedimentary rocks (limestone, shale, and sandstone). River flow is responsible for recent sedimentation in Göksun, caused formation of alluvial plains leading to the formation of extensive alluvial plains over time. Alluvial fans consisting of gravelly and sandy soils are also encountered, where the groundwater table level is quite high. In this regard, a model was established for Göksun by use of geological and geophysical data, and geological cross-section of valley can be seen in Figures 3a and 3b. In Figure 2, the location of station 4612 in Göksun district and the geological context of the district are presented.

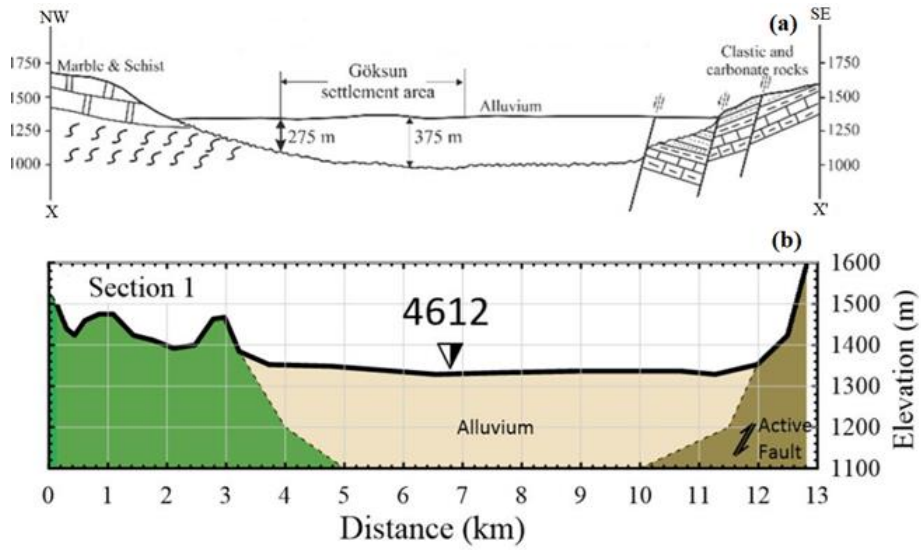

Figure 3. a) Valley section interpreted using geological and seismological data; b) Valley section in the South-East/ North-west direction passing through the station 4612.

3. The February 6, 2023 earthquakes

On 6th of February 2023, eastern Türkiye was shaken by two consecutive earthquakes with moment magnitudes of M_w=7.7 and 7.6 (AFAD, 2023a). The first event, Pazarcik earthquake (M_w=7.7), was triggered by a left-lateral strike-slip fault within the Eastern Anatolian Fault Zone (epicenter Pazarcik, Kahramanmaras, Türkiye – 37.288°N, 37.043°E – focal depth 8.6 km) at 4:17 AM local time (GMT +3). The second event Elbistan earthquake (M_w 7.6), occurred approximately 9 hours later, at 13:24 local time (epicenter Elbistan-Kahramanmaras, Türkiye – 38.089°N, 37.239°E – focal depth 7.0 km). The distribution of the Peak Ground Acceleration (PGA) recorded in southeastern Türkiye and locations of the epicenters are shown in Figure 4.

The first (Pazarcik, Mw=7.7) earthquake was triggered by the Narli segment of the Dead Sea Fault Zone, affecting Celikhan, Golbasi, and Amanos regions, while the second (Elbistan, Mw=7.6) earthquake was associated with the Cardak Fault and the Dogansehir Fault Zone. These seismic events resulted in surface ruptures extending approximately 300 km and 130 km in length, with displacements exceeding 6.5 m, respectively. During the three-month period following the earthquakes, the region experienced a total of 33,591 seismic events ranging in magnitude from 0.2 to 6.6. Among these, 550 earthquakes fell within the 4.0 to 5.0 magnitude range, 48 events fell within the 5.0 to 6.0 magnitude range, and 2 events registered magnitudes between 6.0 and 7.0 (AFAD, 2023a).

The main features of the earthquakes and the damage occurred were reported in literature (Çetin et al., 2023a,b). Many geotechnical problems including surface rupture, ground shaking with very high accelerations, surface and deep cracks, loss in slope stability, liquefaction-induced settlements, rockfalls, and completely destroyed infrastructures. Along with low structural quality of building stock in the area, these events caused significant death toll and loss in property.

As reported in Figure 4, it is possible to notice high values of PGA around Göksun after the Elbistan earthquake (Figure 4b), even though the city is not in the epicentral area. No similar anomalies can be observed in the case of the first event (Figure 4a).

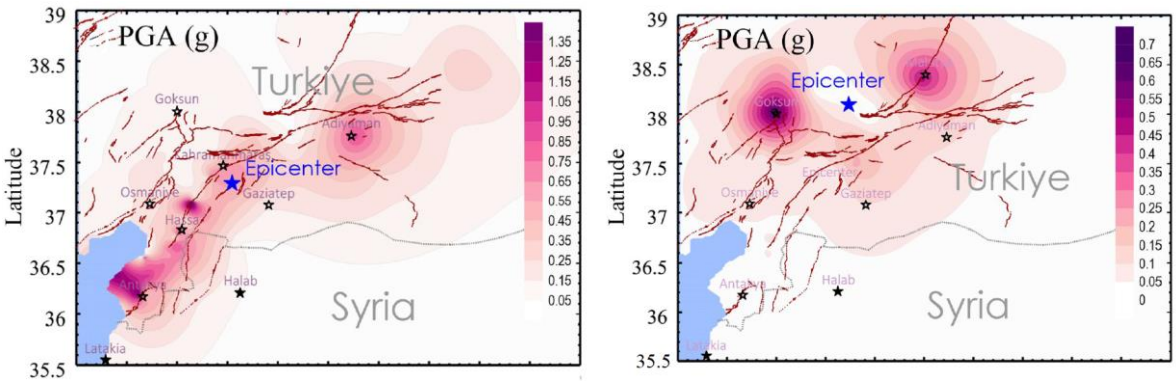

(a) (b)

Figure 4. Epicenters of the a) Pazarcik and b) Elbistan seismic events and location of the Göksun city.

3.1. Observed damage in Göksun district

After the earthquakes, a significant structural damage was observed in many of the historical buildings, infrastructure systems, and many residences in the Göksun district. As could be observed from distribution of PGA in the region, concentration of ground accelerations were in the vicinity of Göksun city.

As expected, damage was mostly occurred after the second event. It should be noted that more than 650 buildings were collapsed during the earthquakes, and more than six thousand buildings will be reconstructed, after their demolition. Also, loss in slope stability and deep cracks were observed in rural districts (Figure 5).

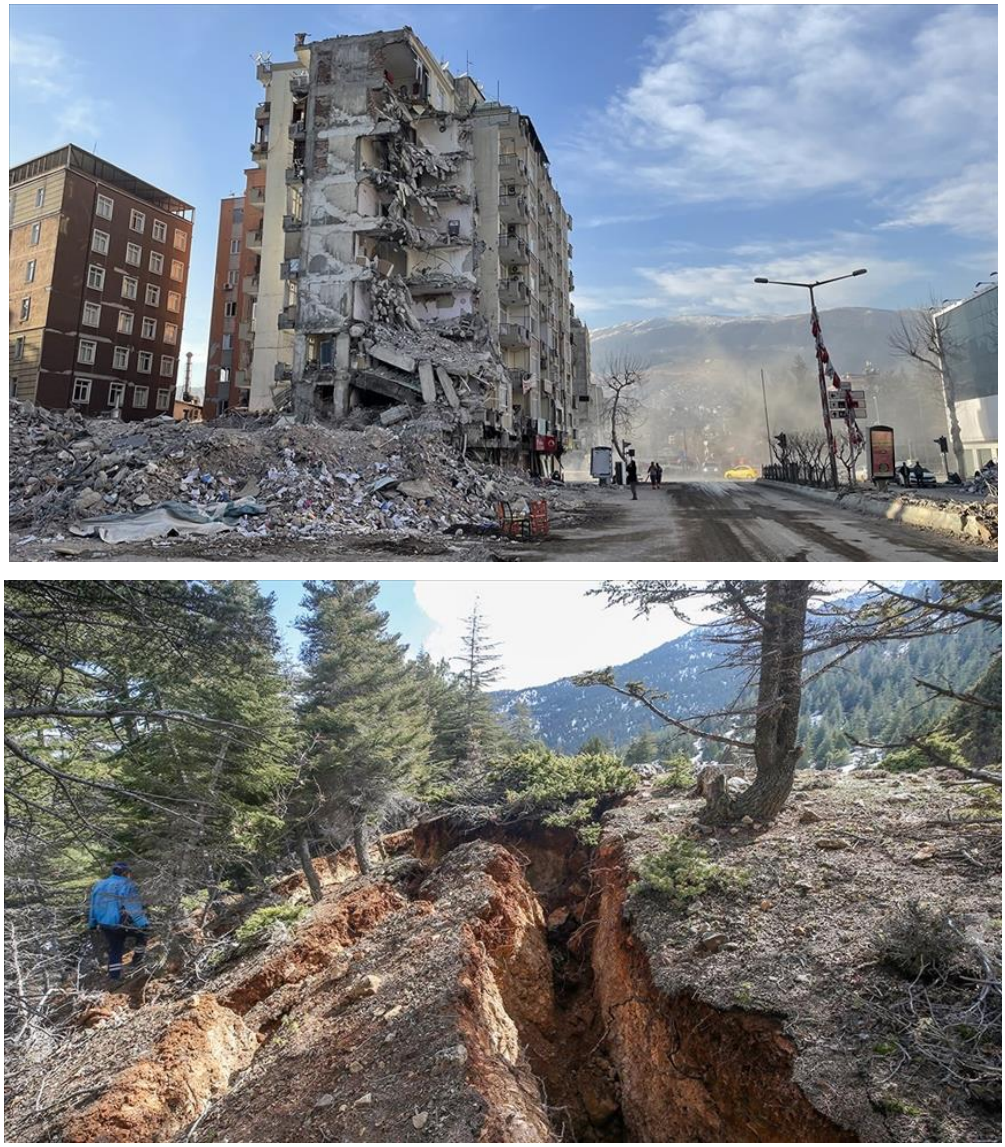

Figure 5. Observed damage in Göksun city (Photos from Anadolu Ajans, https://www.aa.com.tr/tr/asrin-felaketi/kahramanmarasin-Göksun-ilcesinde-5-1-buyuklugunde-deprem-/2824289, https://www.aa.com.tr/tr/asrin-felaketi/Göksunda-deprem-nedeniyle-derin-yariklar-olustu/2837685).

3.2. Ground motion distribution

A maximum acceleration of 0.143 g was recorded in station 4612 approximately 100 km northwest of the epicenter of the first earthquake. Information obtained from AFAD (2023b) reveal that this station is located over Class C soil deposit, ($V_{s,30}$=246 m/s). On the other hand, station 0129, located 135 km from the epicenter and close to rock formations with $V_{s,30}$=965 m/s, recorded a maximum acceleration of roughly 0.05 g (Figure 6). During the first event, significant damage was reported. In the second event (the Elbistan earthquake), the highest accelerations were recorded in Göksun. Stations 4612 and 0129 were located approximately 67 and 91 km from the event epicenter of second event, respectively. The maximum accelerations recorded at Stations 4612 and 0129 were 0.65 g and 0.17 g, respectively.

Figure 6 presents the contours of $S_{a(0.3s)}$ of Elbistan (M_w=7.6) of Göksun City and its periphery. This figure also includes the locations of the strong-motion stations and active faults. The high accelerations are concentrated around Göksun city center, where the map indicates that the valley appears to be boosted. The maximum spectral acceleration, $S_{a(0.3s)}$, in this region was approximately 0.9 g. Wu et al. (2023) stressed that no pulse-like ground motion was identified. Therefore, the wave attenuation during Elbistan event agrees with ordinary GMPE, in contrast to the first (Pazarcik) earthquake.

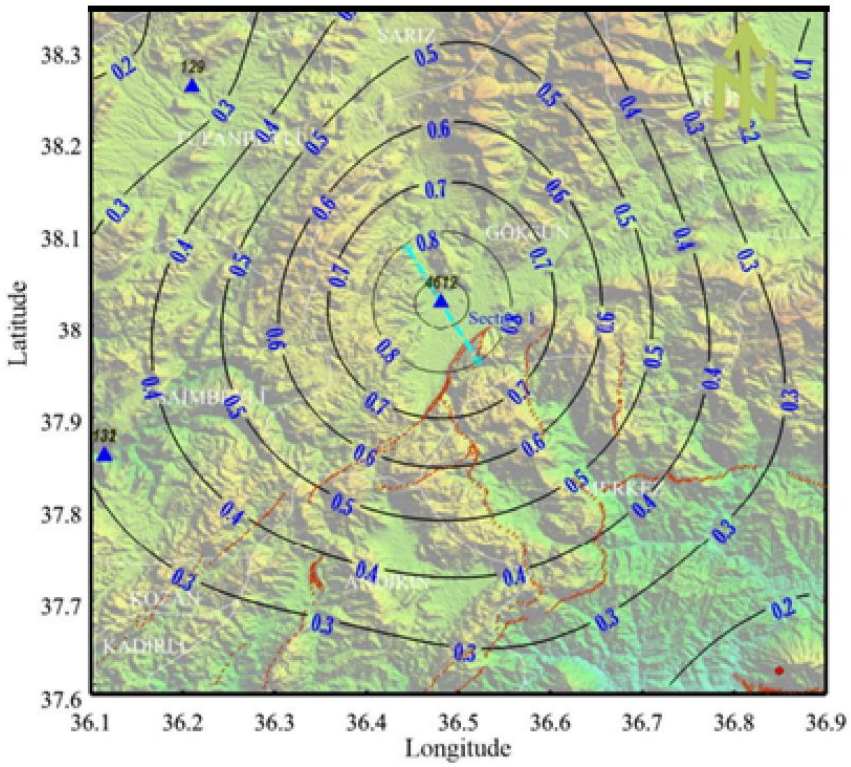

Figure 6. Contours of spectral acceleration $S_{a\ (T=0.3s)}$ of February 2023 Elbistan M_w=7.6 earthquake on the background map of Göksun region.

Spectra obtained from analysis of records in 4612 and 0129 stations reveal a remarkable amplification of motion particularly for periods exceeding 0.2 s. The response spectra exhibit prominent peaks at 1.6 s, proving that the thicknesses of deposits in interpreted section is higher than 120 m. This observation aligns with the findings of the geological cross-section, as depicted in the north-west to south-east directional geological cross-section in Figure 4a. As shown in Figure 5a, the thickness of the alluvial deposits varies between 275 m and 375 m below the area of Göksun. Table 1 presents the recorded PGA around Göksun. The information can be used to understand the difference among rock and soil PGA observations.

Table 1. Recorded PGA (g) at the recording stations around Göksun.

Recording station	**Equivalent Shear wave velocity (m/s)**	**Subsoil class**	**PGA (g)**
0129	965	A	0.05
4612	246	C	0.65

The variations in spectral accelerations, as computed using data from stations 4612 and 0129, are graphically depicted in Figure 7. Acceleration spectra for damping ratio of 5% were computed for station 4612 and 0129 for both horizontal directions (E-W and N-S) and compared with spectrum of the closest station on the rock (station 0129). In accordance with the Turkish Building Earthquake Code (TBEC, 2018), for a design earthquake ground motion level (DD-1) with a 2% probability of exceedance in 50 years (return period of 2475 years), the horizontal elastic design response spectra specified for ZC soil classes were also compared with the response spectra obtained from both directions. In addition to taking certain precautions in the direct comparison of the spectra of the recorded signals, it is observed that spectral accelerations, especially for periods greater than 1 second, exceed the regulatory limits.

It is important to highlight that the spectral accelerations exhibit a substantial increase, reaching up to 1.4g at station 4612, while at the rock site (station 0129), the increase is limited to 0.4g. Furthermore, the predominant periods obtained from the analyses encompass a range of 0.4 – 2 s. for station 4612 and 0.06 – 0.2 s. for station 0129, respectively. These findings emphasize the presence of site-specific effects, underscoring a prolonged duration of ground shaking. This prolonged shaking is further accentuated by the valley effects experienced in Göksun. These results are in alignment with the geological characteristics of the region, as mentioned earlier.

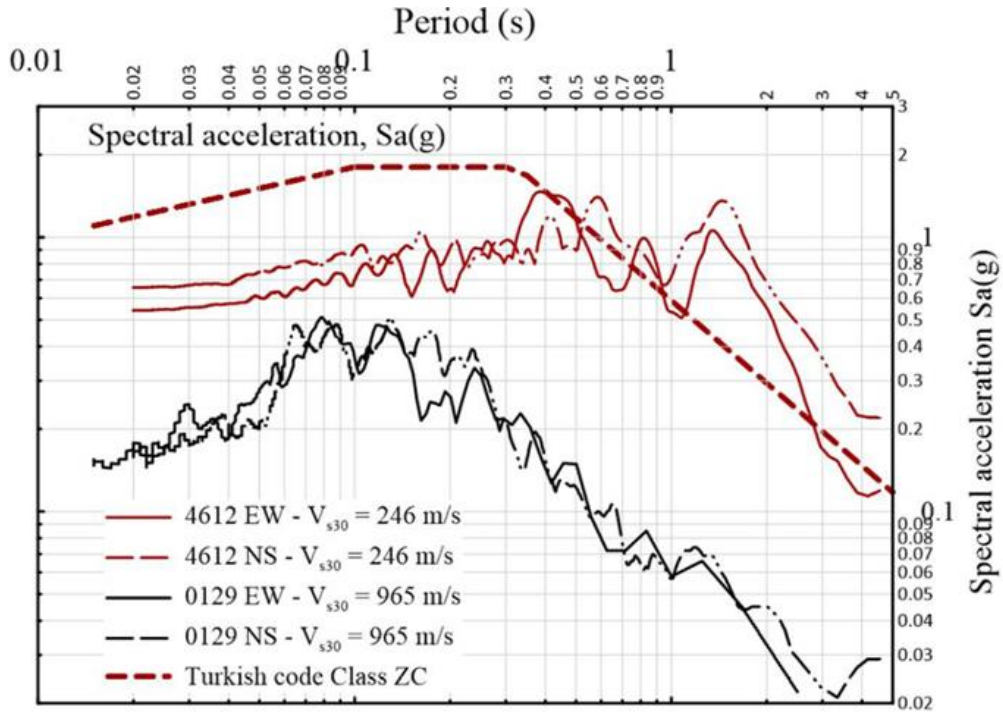

Figure 7. Change in spectral acceleration $S_{a\ (T=0.3s)}$ in stations 0129 and 4612 after February 2023 Elbistan M_w=7.6 earthquake

4. Conclusions

Two consecutive events caused massive damage and life losses in eastern Türkiye. This study is an attempt to summarize the relevance among geological and geotechnical factors that have combined to produce accelerations rarely seen in similar events around the world. In the Göksun region, which is one of the most severely affected areas by the Elbistan earthquake and situated within a deep alluvial valley, it is evident that site effects play a significant role in amplifying ground motions, with acceleration intensity becoming increasingly pronounced as the period increases. The presence of sedimentary rocks such as limestone, shale, and sandstone, coupled with the substantial thickness of alluvial deposits, results in amplified ground motion, especially for longer periods.

In the analysis, the response spectra show peaks at a period of approximately 1.6 s., which is proof of deposit thickness higher than 275 m. For periods greater than 0.2 seconds, significant amplifications were observed. This amplification effect was particularly pronounced during the second seismic event, with the peak ground acceleration (PGA) exhibiting a notable concentration in the Göksun city and its periphery. During the reconnaissance studies, personal communications by Eyyüb Karakan revealed that the damage in the city dominantly occurred after the second event, which aligns with the concentration of PGA during Elbistan earthquake.

Notably, these accelerations were generally much higher than existing design spectra. Concentration of damage was found to be correlated with amplification due to local soil conditions. Notably, these data indicates that the geological context of the region plays a crucial role in shaping the seismic response. the observable

valley effects were found to play a significant role and could account for the significant damage observed in this area.

In conclusion, the seismic events that occurred in Göksun on 6th of February 2023, shed light on the paramount importance of considering site-specific effects in seismic risk assessments and infrastructure planning. The findings from this study unequivocally underline the pronounced influence of local geological conditions on ground motions, which, in turn, significantly impact the structural integrity of buildings and infrastructure. Given these findings, it is imperative that future seismic risk assessments, infrastructure designs, and land-use planning in Göksun and similar regions consider the profound implications of site-specific geological and hydrogeological factors.

The results obtained from this study, aimed at understanding the ground motion distribution and soil effects of major earthquakes occurring in Pazarcik and Elbistan, provide valuable information that will be utilized in future research to implement precautionary measures in earthquake-prone regions and enhance structural resilience. This will be instrumental in reducing earthquake-related damage, safeguarding lives, and promoting the resilience of the built environment in the face of seismic events. Future developments of the study will include two-dimensional and three-dimensional numerical analyses of the Göksun valley based on the acquisition of results of detailed geotechnical and seismological studies.

5. References

AFAD (2023a). Press Bulletin-36 about the Earthquake in Kahramanmaraş, https://en.afad.gov.tr/press-bulletin-36-about-the-earthquake-in-kahramanmaras, (accessed 18 May 2023), Ankara.

AFAD. (2023b). Republic of Türkiye Ministry of Interior Disaster and Emergency Management Presidency Department of Earthquake Turkish Accelerometric Database and Analysis System.

Asimaki, D., Mohammadi, K., Mason, H. B., Adams, R. K., Rajaure, S., Khadka, D. (2017). Observations and Simulations of Basin Effects in the Kathmandu Valley during the 2015 Gorkha, Nepal, Earthquake Sequence. Earthquake Spectra, 33, 35–53. https://doi.org/10.1193/013117eqs022m.

Bard, P-Y., & Bouchon, M. (1985). The two-dimensional resonance of sediment-filled valleys. Bulletin of the Seismological Society of America, 75(2), 519–541. https://doi.org/10.1785/BSSA0750020519.

Bard, P-Y., & Bouchon, M. (1980a). The seismic response of sediment-filled valleys. Part 1. The case of incident SH waves. Bulletin of the Seismological Society of America, 70(4), 1263–1286. https://doi.org/10.1785/BSSA0700041263.

Bard, P-Y., & Bouchon, M. (1980b). The seismic response of sediment-filled valleys. Part 2. The case of incident P and SV waves. Bulletin of the Seismological Society of America, 70(5), 1921–1941. https://doi.org/10.1785/BSSA0700051921.

Bielak, J., Xu, J., & Ghattas, O. (1999). Earthquake Ground Motion and Structural Response in Alluvial Valleys. Journal of Geotechnical and Geoenvironmental Engineering, 125(5), 413-423. https://doi.org/10.1061/(ASCE)1090-0241(1999)125:5(413).

Çetin, KO., Altun, S., Askan, A., Akgün, M., Sezer, A., Kıncal, C., et al. (2022). The site effects in Izmir Bay of October 30, 2020, M7.0 Samos Earthquake. Soil Dynamics and Earthquake Engineering, 152, 107051. https://doi.org/10.1016/j.soildyn.2021.107051.

Çetin, K.O., Papadimitriou, A.G., Altun, S., Pelekis, P., Unutmaz, B., Rovithis, E., et al. (2022). The role of site effects on elevated seismic demands and corollary structural damage during the October 30, 2020, M7.0 Samos Island (Aegean Sea) Earthquake. Bulletin of Earthquake Engineering, 20, 7763–92.https://doi.org/10.1007/s10518-021-01265-z.

Çetin KÖ, et al. (2023a). Reconnaissance report on February 6, 2023 Kahramanmaraş-Pazarcık (Mw=7.7) and Elbistan (Mw=7.6) Earthquakes. Ankara.

Çetin KÖ, Bray JD, Frost JD, Hortacsu A, Miranda E, Moss RES, et al. (2023b). February 6, 2023 Türkiye Earthquakes: Report on Geoscience and Engineering Impacts.

Chiaradonna A, Karakan E, Kincal C, Lanzo G, Monaco P, Sezer A, et al. (2023). Insights on the role of local site effects on damage distribution in the Izmir metropolitan area induced by the October 30, 2020 Samos earthquake. Soils and Foundations, 63, 101330. https://doi.org/10.1016/j.sandf.2023.101330.

Emre, Ö., Duman, T. Y., Özalp, S., Elmacı, H., Olgun, Ş. & Şaroğlu, F. (2013). Active Fault Map of Türkiye with and Explanatory Text. General Directorate of Mineral Research and Exploration (MTA), Special Publication Series, 30, Ankara- Türkiye.

Garini E, Anastasopoulos I, Gazetas G. (2020). Soil, basin and soil–building–soil interaction effects on motions of Mexico City during seven earthquakes. Géotechnique, 70, 581–607. https://doi.org/10.1680/jgeot.18.P.314.

Google Earth Pro. Göksun. 280100/4210417.1352 m. 2023.

Graves RW. (1993). Modeling three-dimensional site response effects in the Marina District Basin, San Francisco, California. Bulletin of the Seismological Society of America, 83, 1042–63. https://doi.org/10.1785/BSSA0830041042.

Ilbank General Directorate (2010). Geotechnical survey report of areas requiring geotechnical survey based on the revised zoning plan of Göksun Municipality, ILB-I/46.018.003.

Makra K, Rovithis E, Riga E, Raptakis D, Pitilakis K. (2021). Amplification features and observed damages in İzmir (Türkiye) due to 2020 Samos (Aegean Sea) earthquake: identifying basin effects and design requirements. Bulletin of Earthquake Engineering, 19, 4773–804. https://doi.org/10.1007/s10518-021-01148-3.

Pagliaroli A, Aprile V, Chamlagain D, Lanzo G, Poovarodom N. (2018). Assessment of site effects in the Kathmandu valley, Nepal, during the 2015 Mw 7.8 Gorkha earthquake sequence. Engineering Geology, 239, 50–62. https://doi.org/10.1016/j.enggeo.2018.03.011.

Papageorgiou AS, Kim J. (1991). Study of the propagation and amplification of seismic waves in Caracas Valley with reference to the 29 July 1967 earthquake: SH waves. Bulletin of the Seismological Society of America, 81, 2214–33.

Presidency of Disaster and Emergency Management (AFAD) (2018). Turkish Building Earthquake Code.

Seed HB, Whitman RV, Dezfulian H, Dobry R, Idriss IM. (1972). Soil conditions and building damage in 1967 Caracas earthquake. Journal of Soil Mechanics and Foundation Engineering, 98, 787–806.

Seed HB, Romo MP, Sun JI, Jaime A, Lysmer J. (1988). The Mexico Earthquake of September 19, 1985—Relationships between Soil Conditions and Earthquake Ground Motions. Earthquake Spectra, 4, 687–729. https://doi.org/10.1193/1.1585498.

Stephenson WRB, Benites RA, Davenport PN. (2009). Localized coherent response of the La Molina basin (Lima, Peru) to earthquakes, and future approaches suggested by Parkway basin (New Zealand) experience. Soil Dynamics and Earthquake Engineering, 29, 1347–57. https://doi.org/10.1016/j.soildyn.2009.05.002.

Wu F, Xie J, An Z, Lyu C, Taymaz T, Irmak TS, et al. (2023). Pulse-like ground motion observed during the 6 February 2023 MW7.8 Pazarcık Earthquake (Kahramanmaraş, SE Türkiye). Earthquake Science, 36, 328–39. https://doi.org/10.1016/j.eqs.2023.05.005.

Yegian MK, Ghahraman VG, Gazetas G. (1994). Ground‐Motion and Soil‐Response Analyses for Leninakan, 1988 Armenia Earthquake. Journal of Geotechnical Engineering, 120, 330‐48.. https://doi.org/10.1061/(ASCE)0733-9410(1994)120:2(330).

Zahradnik J, From H. (1987). Seismic Ground motion of Sedimentary Valleys-Example La Molina, Lime, Peru. Journal of Geophysics, 62, 31–7.

Zhang B, Papageorgiou AS. (1996). Simulation of the response of the Marina District Basin, San Francisco, California, to the 1989 Loma Prieta earthquake. Bulletin of the Seismological Society of America, 86, 1382–400.